Published OnlineFirst October 2, 2013; DOI: 10.1158/2159-8290.CD-13-0186

RESEARCH ARTICLE

A Chimeric RNA Characteristic of Rhabdomyosarcoma in Normal Myogenesis Process

Huiling Yuan[1], Fujun Qin[1], Mercedeh Movassagh[1], Hong Park[1], Wendy Golden[1], Zhongqiu Xie[1], Peng Zhang[1], Jeffrey Sklar[3], and Hui Li[1,2]

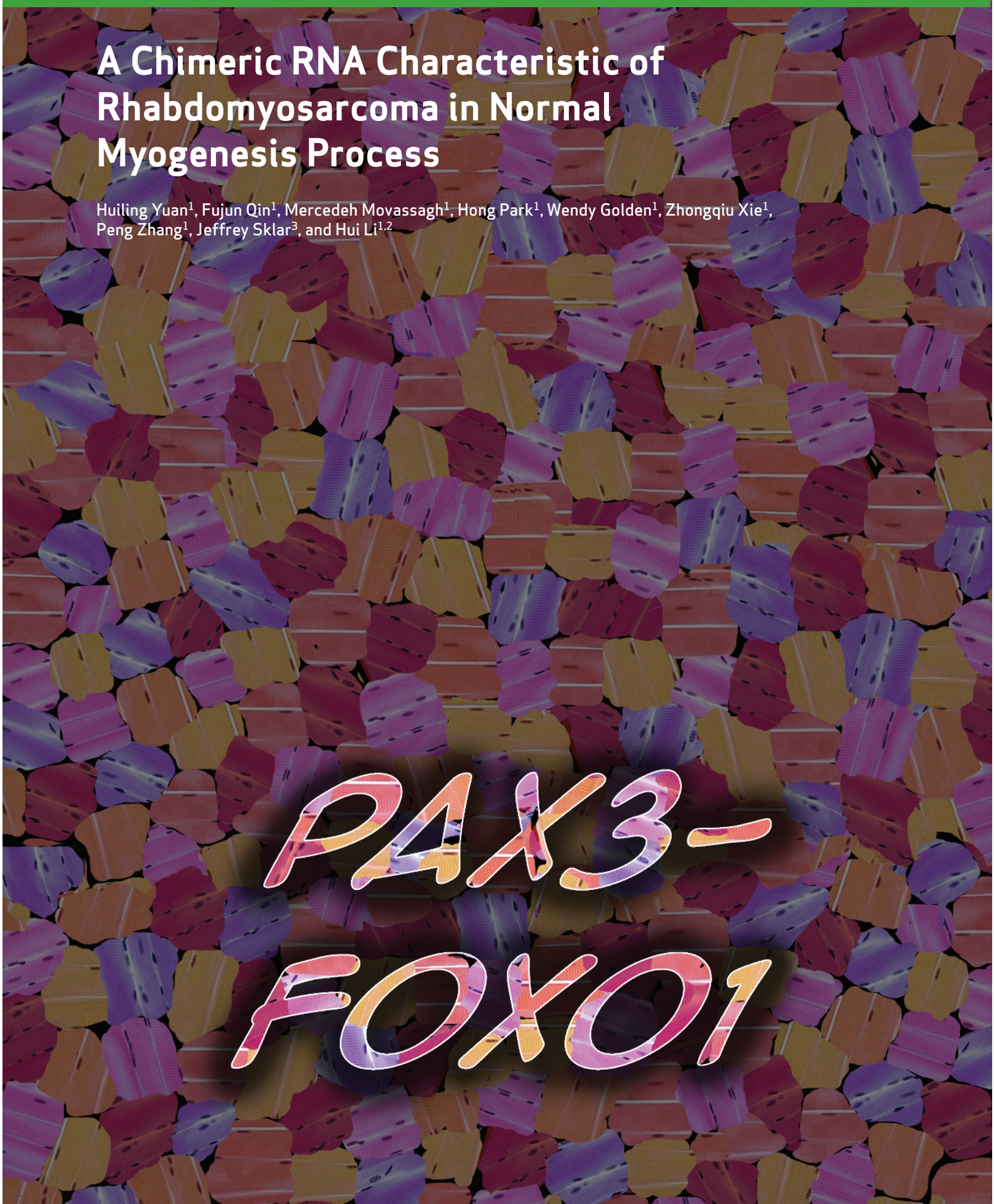

Published OnlineFirst October 2, 2013; DOI: 10.1158/2159-8290.CD-13-0186

ABSTRACT Gene fusions and their chimeric products are common features of neoplasia. Given that many cancers arise by the dysregulated recapitulation of processes in normal development, we hypothesized that comparable chimeric gene products may exist in normal cells. Here, we show that a chimeric RNA, *PAX3–FOXO1*, identical to that found in alveolar rhabdomyosarcoma, is transiently present in cells undergoing differentiation from pluripotent cells into skeletal muscle. Unlike cells of rhabdomyosarcoma, these cells do not seem to harbor the t(2;13) chromosomal translocation. Importantly, both *PAX3–FOXO1* RNA and protein could be detected in the samples of normal fetal muscle. Overexpression of the chimera led to continuous expression of MYOD and MYOG—two myogenic markers that are overexpressed in rhabdomyosarcoma cells. Our results are consistent with a developmental role of a specific chimeric RNA generated in normal cells without the corresponding chromosomal rearrangement at the DNA level seen in neoplastic cells presumably of the same lineage.

SIGNIFICANCE: A chimeric fusion RNA, *PAX3–FOXO1*, associated with alveolar rhabdomyosarcoma, is also present in normal non-cancer cells and tissues. Its transient expression nature and the absence of t(2;13) chromosomal translocation are consistent with a posttranscriptional mechanism. When constantly expressed, PAX3–FOXO1 interfered with the muscle differentiation process, which presumably contributes to tumorigenesis. *Cancer Discov; 3(12); 1394–1403. ©2013 AACR.*

INTRODUCTION

Gene fusions resulting from chromosomal rearrangements and most often interchromosomal translocations are considered a genetic hallmark of many neoplasias (1, 2). Specific head-to-tail fusions of two genes are generally characteristic of individual subtypes of tumors and have become important diagnostic markers over the last several decades. As has been demonstrated by abundant experimental evidence, these chimeric products arising from these fusions are most often causally related to the neoplastic behavior of the cells and tumors containing them. Recently, we discovered in normal endometrial cells a form of chimeric mRNA and protein identical to that found in endometrial stromal sarcomas (3). In normal endometrial stroma, this RNA seems to result from *trans*-splicing between precursor mRNAs transcribed from the two intact genes *JAZF1* and *JJAZ1* (also called *SUZ12*; ref. 3). On the basis of these findings, we hypothesized that at least some chimeric RNAs are present in certain normal cells of a tissue and play normal physiologic functions in those cells, and that gene fusions in neoplastic cells may produce the chimeras in a constitutive and unregulated fashion. Because the chimeric proteins translated from these RNAs are oncogenic, we speculated that chimeric RNAs in normal cells appear only under certain conditions, for limited periods of time, and/or at low levels. In addition, such chimeric RNAs may be produced in the absence of chromosomal rearrangement in normal cells. Besides *JAZF1–JJAZ1*, reports for other chimeric RNAs generated by non-chromosomal rearrangement mechanisms are also emerging. Recently, reciprocal RNA chimera involving *YPEL5* and *PPP1CB* was identified by transcriptome sequencing, and no corresponding rearrangement at the DNA level was found (4). In addition, we reported *cis*-splicing of adjacent genes as another mechanism to generate *SLC45A3–ELK4* chimera involving neighboring genes transcribing in the same direction (5).

RESULTS

To test the hypothesis, we monitored normal bone marrow–derived mesenchymal stem cells (MSC) induced to differentiate along the skeletal muscle lineage for expression of the chimeric RNA *PAX3–FOXO1*, which is transcribed from a gene fusion found in over half the cases of alveolar rhabdomyosarcoma (ARMS), a soft-tissue sarcoma of children and young adults (6, 7). Expression of *PAX3–FOXO1* RNA could be detected transiently along the differentiation process, and the expression of *PAX3–FOXO1* preceded the expression of myogenic early stage markers (*MYOD* and *MYOG*; Fig. 1A). Similar muscle differentiation studies were performed using another source of adult stem cells, adipose-derived stem cells (ASC) isolated from fat tissue removed by liposuction. In a representative study (total $n = 3$), *PAX3–FOXO1* fusion RNA was detected at only one time point, day 8 (Fig. 1B). As in the prior studies with bone marrow MSCs, the expression of *PAX3–FOXO1* preceded the expression of *MYOD* and *MYOG* mRNA. Sequencing analysis revealed that the chimeric RNA detected during the differentiation was identical to the

Authors' Affiliations: [1]Department of Pathology and [2]University of Virginia Cancer Center, University of Virginia, Charlottesville, Virginia; and [3]Department of Pathology, Yale University, New Haven, Connecticut

Note: Supplementary data for this article are available at Cancer Discovery Online (http://cancerdiscovery.aacrjournals.org/).

Current address for H. Yuan: Department of Breast Surgery, Dongguan People's Hospital, Dongguan, Guangdong, China.

Corresponding Author: Hui Li, Department of Pathology and Cancer Center, University of Virginia, 345 Crispell Drive, MR6-B524, Charlottesville, VA 22908. Phone: 434-982-6680; Fax: 434-243-7244; E-mail: hl9r@virginia.edu

doi: 10.1158/2159-8290.CD-13-0186

Published OnlineFirst October 2, 2013; DOI: 10.1158/2159-8290.CD-13-0186

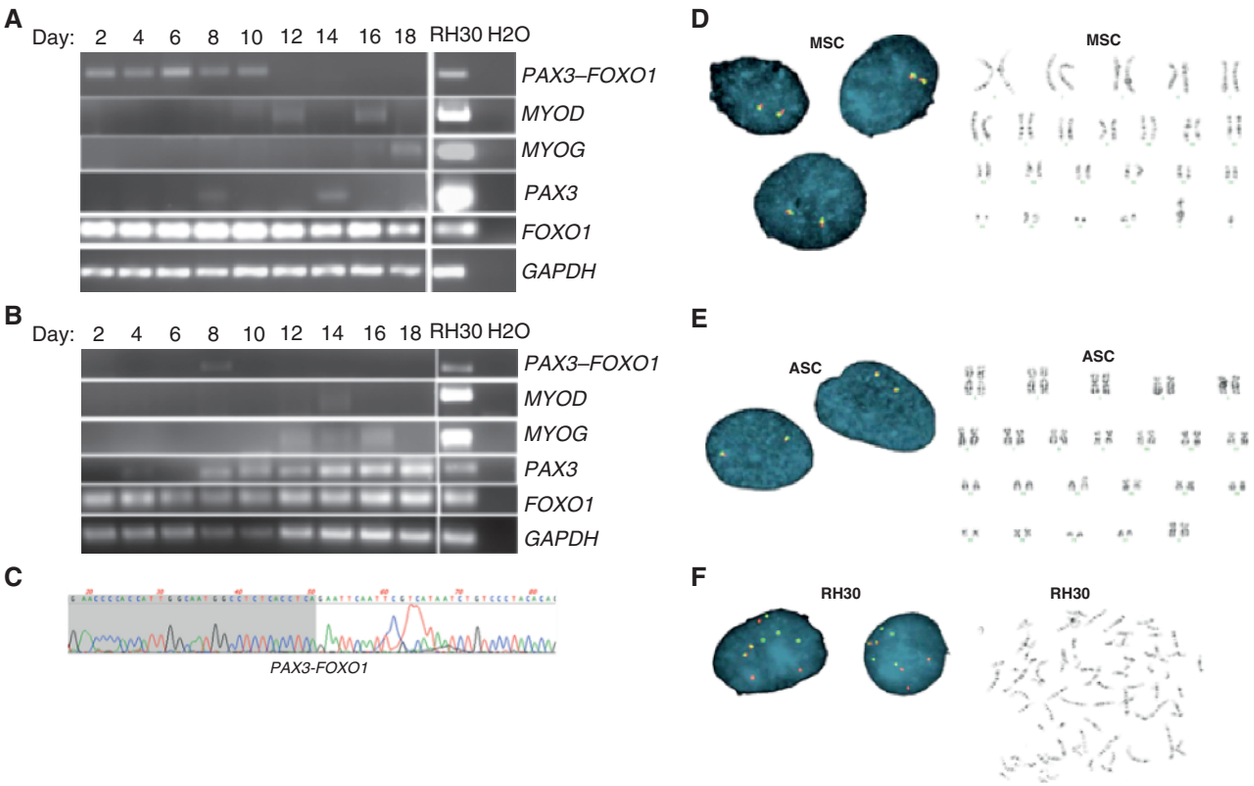

Figure 1. Detection of *PAX3-FOXO1* RNA during muscle differentiation and absence of chromosomal translocation in these cells. A representative of multiple repeats ($n > 3$) is shown. Bone marrow MSCs (**A**) or ASCs (**B**) were induced to differentiate along a skeletal muscle lineage. RNA was extracted from samples harvested every other day from day 2 to day 18. *PAX3–FOXO1*, *MYOD*, and *MYOG* RNAs were assessed by RT-PCR. RNA from the rhabdomyosarcoma cell line RH30 was used as positive control. **C,** sequencing analysis of the above *PAX3–FOXO1* reverse transcription PCR products revealed a nucleotide sequence at the *PAX3–FOXO1* junction identical to the product generated from chromosomal translocation in alveolar rhabdomyosarcoma. **D–F,** FISH and cytogenetic analysis in bone marrow MSCs (**D**), ASCs (**E**), and RH30 (**F**). FISH was performed using a *FOXO1* Dual Color Break-Apart FISH probe Kit. Karyotyping analysis was done as described in Methods.

PAX3–FOXO1 RNA found in ARMS (first 7 exons of *PAX3* joined to last 2 exons of *FOXO1*; Fig. 1C). Because of the stochastic nature of muscle differentiation *in vitro*, the exact time point of *PAX3–FOXO1* expression varied in multiple repeating experiments, and sometimes another wave of expression was observed after the initial transient expression. However, *PAX3–FOXO1* always preceded the expression of *MYOD* and *MYOG* (Supplementary Fig. S1). In longer-term differentiation settings (28 days), Myosin heavy chain (*MYH*) transcript (Supplementary Fig. S1A and S1B) and MYH protein (Supplementary Fig. S2A) were also detected, along with another feature of terminal skeletal muscle formation, multi-nucleation (Supplementary Fig. S2B).

These adult stem cells from bone marrow and fat used in our studies were obtained from healthy non-cancer donors and contained normal numbers of chromosomes and G banding patterns in cytogenetic analyses (Fig. 1D and E). In contrast, the ARMS cell line RH30 showed abnormal chromosomal banding and aneuploidy (Fig. 1F). To further confirm the absence in these normal cells of the t(2;13)(q35;q14) chromosomal translocation that produces the *PAX3–FOXO1* fusion in ARMS, we used a clinically used diagnostic FISH kit for ARMS to detect recombination at the *FOXO1* locus. A total of 200 cells from each of both stem cell cultures were scored. No separation of red and green signals was observed in the two types of stem cell cultures (Fig. 1D and E), indicating the absence of a translocation involving *FOXO1*. However, separation of multiple unpaired red and green fluorescence signals was seen in RH30 cells (Fig. 1F), consistent with the previous finding that this cell line has a complex karyotype with amplification of the fusion gene (8).

The timing of generation of *PAX3–FOXO1* RNA did not correlate with that of wild-type *PAX3* or *FOXO1* RNA during the process, arguing against the possibility of nonspecific splicing due to high levels of wild-type transcripts. To further confirm this finding, we developed quantitative PCR (qPCR) assays to measure the chimera and wild-type *PAX3* (primers spanning intron 7) and *FOXO1* (primers spanning intron 1) expression (Supplementary Fig. S3). No correlation of the fusion expression level with either wild-type transcript was observed. In addition, no reciprocal *FOXO1–PAX3* chimeric RNA was detected in the muscle differentiation samples, even though it is quite abundant in RH30.

We next investigated whether results obtained with cultured cells also occur *in vivo* during normal muscle development. We macrodissected muscle from sections of formalin-fixed, paraffin-embedded (FFPE) tissue from nine fetal abortuses that resulted from miscarriage or therapeutic abortion due to

Published OnlineFirst October 2, 2013; DOI: 10.1158/2159-8290.CD-13-0186

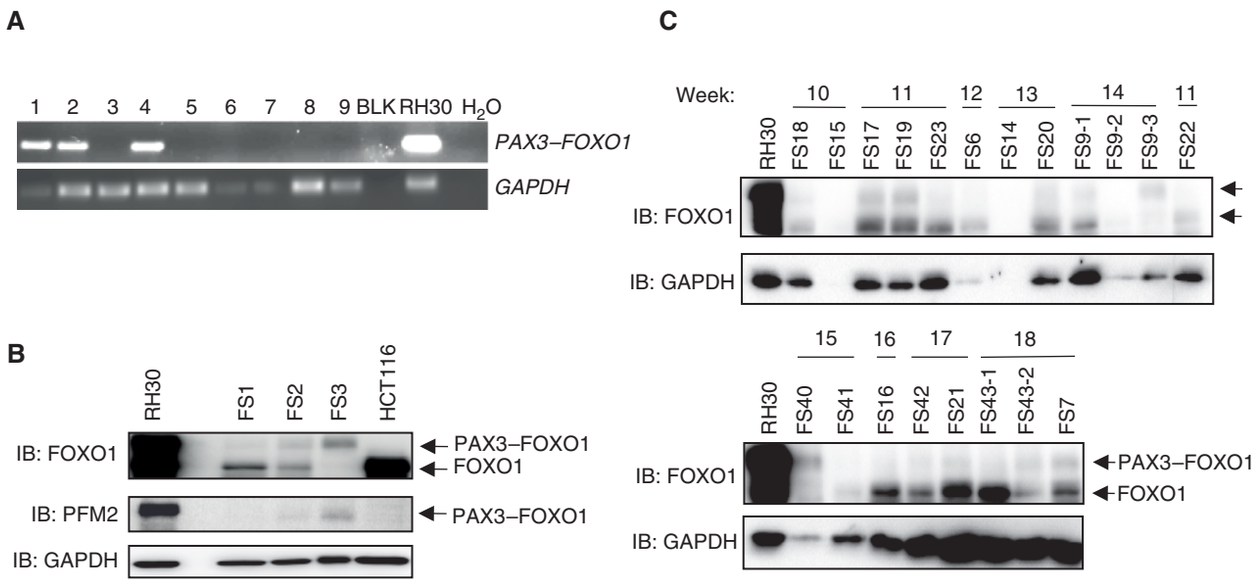

Figure 2. Detection of *PAX3–FOXO1* RNA and protein in human fetal samples. **A,** Total RNAs were extracted from 9 FFPE human fetal tissues and RT-PCR was performed to detect *PAX3–FOXO1* transcript. Lane 1, ARMS control; lane 4, trisomy 18; lane 7, trisomy 21; lanes 2–9, normal karyotype; lane 10, blank paraffin. *GAPDH* RNA was set up as internal control for total RNA input and integrity. **B,** total cellular protein was extracted from samples of three frozen normal abortuses. Western blot analysis was performed using FOXO1 or PFM2 antibodies. Protein from the colon cancer cell line HCT116 was used as a negative control. GAPDH was used as a loading control. **C,** total protein was extracted from 17 fresh-frozen tissue samples of 14 fetuses. Western blot analysis was performed using a FOXO1 antibody. GAPDH, glyceraldehyde-3-phosphate dehydrogenase.

placental previa or trisomy 18 or 21 (one case each). None of the fetuses from which the tissue was obtained showed abnormalities of chromosomes 2 or 13. Chimeric *PAX3–FOXO1* RNA was detected in muscle tissues from two of these cases (Fig. 2A). The PCR products were cloned and Sanger sequencing revealed identical sequence to that of *PAX3–FOXO1* in RH30 cells.

Protein extracts were prepared from three fresh-frozen normal fetal abortuses. A band identical to PAX3–FOXO1 protein was detected using an antibody against FOXO1 by Western blot analysis in all three cases, but not in the negative control colon cancer cell line HCT116 (Fig. 2B). To further confirm the identity of the band, we performed Western blot analysis on the same set of samples with a PAX3–FOXO1-specific monoclonal antibody (PFM2). The specificity of the antibody has been demonstrated before (9) and further confirmed (Supplementary Fig. S4). Using this antibody, we observed the same-size protein bands in two of these fetal samples (Fig. 2B). The relative intensities of the bands corresponded to those in the FOXO1 antibody Western, even though the PFM2 blot has a much fainter signal. We then collected 17 fresh-frozen tissues from 14 fetuses ranging in gestation age from 10 to 18 weeks. Although some of the samples were heavily fragmented with no recognizable morphology, complicating the dissection of muscle tissues, PAX3–FOXO1 protein could be detected in most samples, with no obvious correlation with gestation stage (Fig. 2C). Similar to the observations with RNA in differentiating stem cell cultures, the detection of PAX3–FOXO1 protein mostly did not correlate with the level of wild-type full-length FOXO1 protein, which was below the level of detection in several of the samples positive for PAX3–FOXO1 protein.

To further confirm the presence of the fusion transcript in the fetal samples, and to avoid potential artifacts caused by RT-PCR, we applied a NanoString nCounter technology, which uses unique color-coded molecular barcodes that hybridize directly to multiple target transcripts without reverse transcription and PCR amplification (10). In this system, each capture probe and reporter probe together query a contiguous 100 bp or so region. For fusion RNA targets, we designed the capture probe targeting primarily the sequence 5′ to the fusion junction site, and reporter probe targeting the other side. Together, the probes are specific for the fusion, as either of the two wild-type transcripts will not hybridize to at least one probe. Multiple evidence shown in Fig. 3A suggests that the probe set for *PAX3–FOXO1* is specific: (i) A very strong signal was observed in HEK293 cells transfected with a *PAX3–FOXO1*-expressing plasmid. In contrast, no signal above background was detected in cells transfected with a *PAX3*- or *FOXO1*-expressing plasmid; (ii) a fusion-specific siRNA (11) in RH30 cells caused more than a threefold reduction of the *PAX3–FOXO1* fusion signal; and (iii) a *PAX3–FOXO1* signal was not observed in HESC-597 cells (a cell line expressing a *trans*-spliced *JAZF1–JJAZ1* fusion RNA (3), or in LNCaP cells (expressing *SLC45A3–ELK4* RNA caused by *cis*-splicing of adjacent genes; ref. 5). Using this probe set, two samples with stronger signals in the Western blot analysis (FS17 and FS40) were also positive by nCounter. Samples from ASC and MSC differentiation time points that were positive for the fusion by RT-PCR (ASC^+ and MSC^+) also had signals above background. Besides *PAX3–FOXO1*, two other fusions associated with Ewing sarcoma (*EWS–FLI1*) and desmoplastic small round cell tumor (*EWS–WT1*) were

Published OnlineFirst October 2, 2013; DOI: 10.1158/2159-8290.CD-13-0186

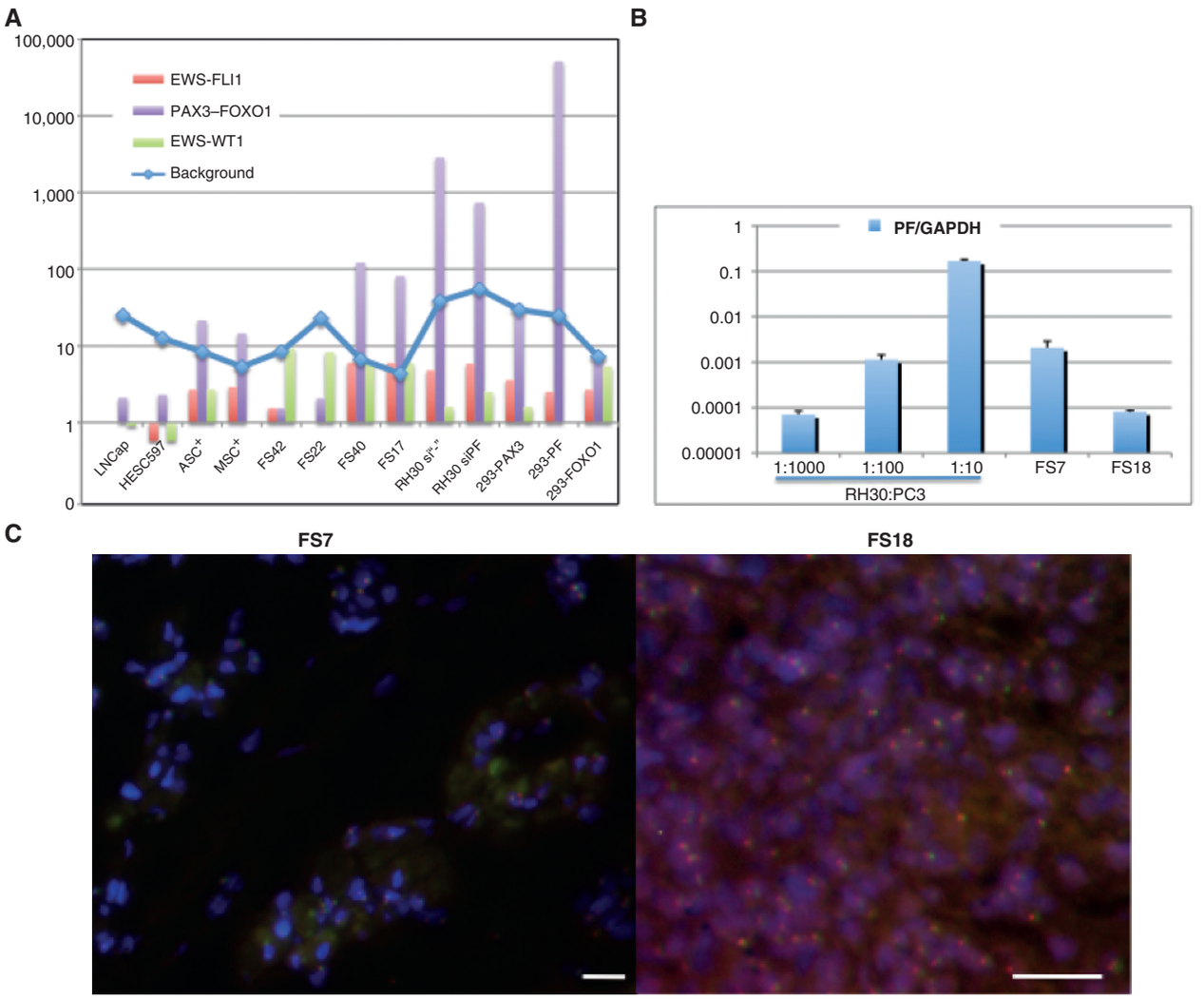

Figure 3. Absence of ARMS-associated chromosomal translocation. **A,** NanoString nCounter assay to detect *PAX3–FOXO1* RNA. RNAs were hybridized to probe sets designed for *PAX3–FOXO1*, *EWS–FLI1*, *EWS–WT1*, and three reference genes, processed and counted by nCounter Digital Analyzer. Testing samples include MSC and ASC RNA samples that were positive by RT-PCR, and four fetal samples that were relatively stronger (FS17 and FS40) or weaker (FS22 and FS42) by Western blot analysis. Controls for *PAX3–FOXO1* probe specificity include 293-PF (293 cells overexpressing the fusion), 293-PAX3 (293 cells overexpressing PAX3), 293-FOXO1 (293 cells overexpressing FOXO1), RH30 si"-" (RH30 cells transfected with negative control siRNA), RH30 siPF (RH30 cells transfected with siRNA targeting the fusion), LNCaP and HESC597 (negative controls). **B,** three continuous frozen sections were cut from FS7 and FS18 samples at a 5-μm thickness. The middle slides of the two samples were subject to RNA extraction and TaqMan qRT-PCR assays to estimate the expression of *PAX3–FOXO1*. Serial dilution of RH30 cells in PC3 prostate cancer cells were used to standards. The chimeric RNA amount was normalized to *GAPDH*. **C,** the top and bottom slides of the two samples were subject to FISH analysis using *FOXO1* break-apart probes. A representative of multiple fields is shown. Scale bar, 30 μm. GAPDH, glyceraldehyde-3-phosphate dehydrogenase.

included as negative controls. None of the samples tested had a signal above background for these two fusions.

Even though all the fetal samples were from non-cancer abortuses, it is still possible that a small percentage of cells harboring t(2;13) is responsible for the *PAX3–FOXO1* signal. In the above NanoString nCounter assay, the signals of *PAX3–FOXO1* in the two fetal samples (FS17 and FS40) are about 3% of that in RH30. To get a better estimate on the expression level of *PAX3–FOXO1* (which reflects the percentage of *PAX3–FOXO1*-expressing cells) in the fetal samples, we used standards with RNA extracted from serial dilutions of RH30 cells in the prostate cancer cell PC3 (negative for *PAX3–FOXO1*) in TaqMan qRT-PCR (Fig. 3B). Three continuous sections were cut at a 5-μm thickness for FS7 and FS18. The middle section was subject to RNA purification and TaqMan qRT-PCR. Assuming that the fusion is expressed at a similar level in fusion-expressing cells in the fetal samples as in RH30 cells, we estimated that the percentage of *PAX3–FOXO1*-expressing cells is about 1% in FS7 and 0.1% in FS18 (Fig. 3B). These numbers may be underestimated, as RH30 cells have several copies of the fusion DNA (Fig. 1F) and they seem to be upregulated. We then performed the FISH analysis with *FOXO1* break-apart probes on the top and bottom sections of each sample. At the 5-μm thickness, 18%–27% of

Published OnlineFirst October 2, 2013; DOI: 10.1158/2159-8290.CD-13-0186

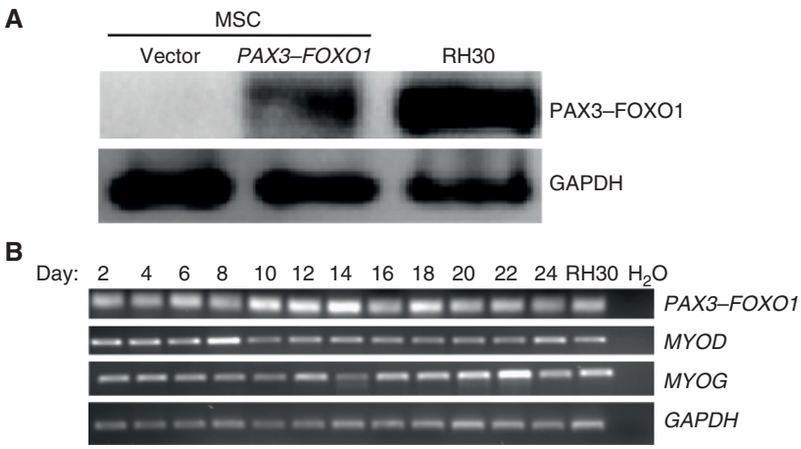

Figure 4. Continuous expression of *MyoD* and *MyoG* induced by constant *PAX3–FOXO1* expression during muscle differentiation. **A,** Similarity in levels of PAX3–FOXO1 protein in MSCs infected with pBabe–PAX3–FOXO1 expression vector as in the ARMS cell line RH30. GAPDH was used as an internal control. **B,** RT-PCR for *PAX3–FOXO1*, *MYOD* and *MYOG* RNA was performed on RNA extracted from MSC cells overexpressing *PAX3–FOXO1* from transducing vectors and harvested every other day from day 2 to day 18. GAPDH, glyceraldehyde-3-phosphate dehydrogenase.

cells have only one pair of signals (Supplementary Fig. S5 and Supplementary Table S1), indicating that a higher percentage of cells were split onto two slides. We scanned multiple fields and scored more than 1,500 cells for each section (1,508 for FS7 top, 2,007 for FS7 bottom, 2,266 for FS18 top, and 1,550 for FS18 bottom). No evidence of *FOXO1* breakage was found (examples in Fig. 3C and Supplementary S6), suggesting the mechanism for the fusion in these cells is unlikely to be chromosomal translocation ($P < 0.001$ for FS7 and $P < 0.05$ for FS18).

The PAX3–FOXO1 fusion protein has greater transcriptional activity than wild-type PAX3 both *in vitro* and *in vivo* (12). Studies in fibroblast and rhabdomyosarcoma cell lines have demonstrated that the PAX3–FOXO1 protein simultaneously induces myogenesis while blocking differentiation to mature muscle, thereby contributing to the formation of ARMS (13, 14). To test the effect of constant expression of PAX3–FOXO1 in the muscle differentiation setting, MSC cells were infected with retroviral vectors that overexpress *PAX3–FOXO1* (Fig. 4A). Under the differentiation condition, *MYOD* and *MYOG* were continuously expressed from day 2 to day 24 in the cells overexpressing *PAX3–FOXO1* (Fig. 4B), in contrast with the transient expression pattern seen in Fig. 1. No mature muscle marker *MYH* expression was observed at any time point when the ectopic fusion was continuously expressed (data not shown), consistent with a role of PAX3–FOXO1 in suppressing terminal differentiation.

We then performed paired-end RNA sequencing (RNA-seq) on MSC samples collected at four different time points [D4, D14, D22 (positive for *PAX3–FOXO1*) and D26], together with RH30. We then used deFuse software (15) to identify fusion RNAs and RT-PCR to validate them. Not surprisingly, the average number of fusions in these normal MSC samples ($n = 7$) is much smaller than that in RH30 ($n = 29$; Fig. 5; Table 1 and Supplementary Table S2). Out of the 30 fusions, 27 were detected only at one time point and three were detected at two time points, suggesting the transient nature of these fusions. Nothing is known about the three fusions, *7SK.206–STX3*, *KDELR1–GRIN2D*, and *RP11-312O7.2–SRGAP2*. However, the fact they were found in MSC D26 as well as in MSC D4 or D14, but not in MSC D22, also supports the wave expression pattern we observed in Supplementary Fig. S1. The majority of the 30 fusions are intrachromosomal, as only three interchromosomal fusions were detected in all the 30 fusions found in MSC samples, including *PAX3–FOXO1*. Consistent with other results presented above, *PAX3–FOXO1* was only transiently detected in MSC D22, and only two other fusions were found in the same sample. None of these two fusions was detected in RH30 cells, further confirming the uniqueness of *PAX3–FOXO1*, which is involved in the particular muscle differentiation stage and in rhabdomyosarcoma. However, one intrachromosomal fusion, *RP11-316I3.1–RP11-316I3.2* was seen in both MSC D26 and RH30, hinting that other fusions may also play a role in both processes.

DISCUSSION

Altogether, these results suggest that the PAX3–FOXO1 fusion product may commit MSCs to the myogenic lineage by transactivating expression of the essential myogenesis factors *MYOD* and *MYOG*. On the other hand, the transience of *PAX3–FOXO1* RNA is consistent with the normal process of muscle differentiation, as prolonged production of *PAX3–FOXO1* RNA leads to constant expression of *MYOD* and *MYOG*, which then blocks terminal differentiation (13, 14). We reasoned that a posttranscriptional process, such as *trans*-splicing of precursor mRNAs, can give rise to transient, temporal appearance of the fusion product (16, 17), whereas gene fusions caused by chromosomal translocation result in constitutive synthesis of chimeric *PAX3–FOXO1* RNA, and in turn *MYOD* and *MYOG* expression that permanently arrests myocytes at immature forms, which can potentially lead to ARMS if combined with secondary mutations. Given the importance of the temporal and kinetic characteristics and patterns of the chimeric expression, we are now developing visualization systems to monitor the expression of the chimera along the muscle differentiation process.

The exact generating mechanism for the fusion is still not clear. The transient expression pattern and the absence of *FOXO1* loci breakage suggest that the fusion is unlikely to be a product of chromosomal translocation. The RNA sequence at the junction is identical to the canonical splicing sites (exon 7 of *PAX3* joined to exon 2 of *FOXO1*), consistent with an RNA *trans*-splicing mechanism. If proven true, *PAX3–FOXO1* will be the second example of a chimeric RNA in normal cells

Published OnlineFirst October 2, 2013; DOI: 10.1158/2159-8290.CD-13-0186

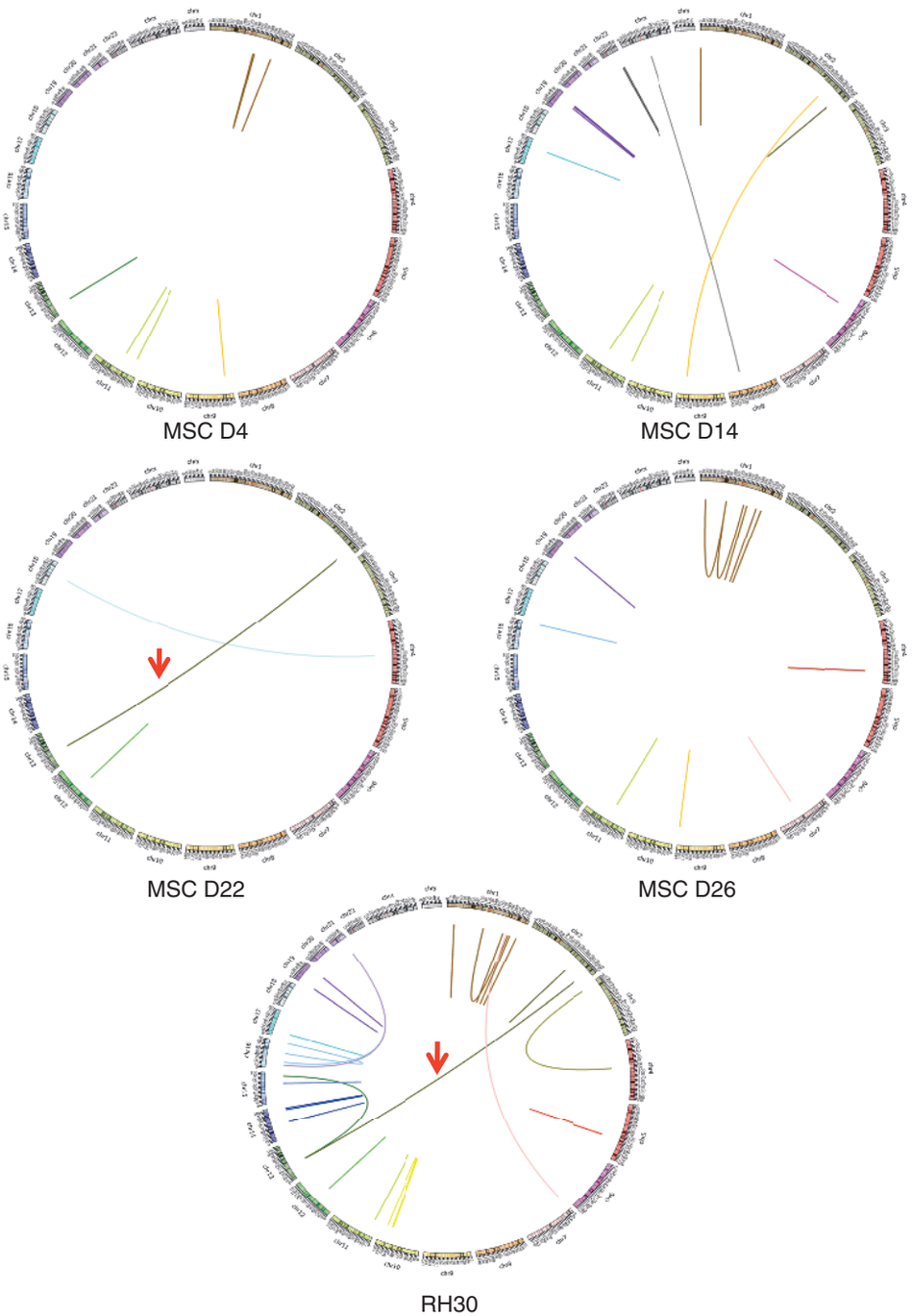

Figure 5. Circos graphic showing the fusions identified through paired-end RNA-seq. Inner circle lines connect two parental genes. Red arrows point to *PAX3–FOXO1* in MSC D22 and RH30.

identical to a gene fusion product in cancer. The mechanism of such intergenic *trans*-splicing is not known. We speculate that it involves the expression and proximity of the parental transcripts. A longer intron tends to facilitate noncanonical splicing. In the case of *PAX3–FOXO1*, *FOXO1* intron 1 is the longest (over 100 kb). However, introns involved in *JAZF1* are not the longest and intron 7 of *PAX3* is also shorter than intron 4. It is also premature to specify other sequence features that are involved in homologous recombination, which may facilitate the fusion RNA generation, at this moment.

The *PAX3–FOXO1* gene fusion is a prominent marker of ARMS and detection of *PAX3–FOXO1* chimeric RNA by RT-PCR is a standard diagnostic procedure (18). Therapies targeting the fusion protein have also been proposed (19). Our findings of the presence of *PAX3–FOXO1* RNA in normal developing muscle samples raise concerns for false positive diagnoses, especially in the sensitive monitoring for residual disease. In addition, therapies targeted at the fusion protein may have side effects due to disruption of functions performed by chimeric *PAX3–FOXO1* RNA in normal developing muscle.

Published OnlineFirst October 2, 2013; DOI: 10.1158/2159-8290.CD-13-0186

Table 1. List of fusions identified through paired-end RNA-seq in MSC samples (D4, D14, D22, and D26)

Sample	gene1_name	gene2_name	gene1_chr	gene2_chr
MSC D4	*RP11-504G3.1*	*UEVLD*	11	11
MSC D4	*7SK.206*	*STX3*	11	11
MSC D4	*RP11-277L2.2*	*PDE4DIP*	1	1
MSC D4	*RP11-312O7.2*	*SRGAP2*	1	1
MSC D4	*MTAP*	*CDKN2B-AS1*	9	9
MSC D4	*RNF17*	*CENPJ*	13	13
MSC D14	*UBE2J2*	*FAM132A*	1	1
MSC D14	*TOMM40*	*APOE*	19	19
MSC D14	*Z82214.1*	*TTLL12*	22	22
MSC D14	*USP32*	*APPBP2*	17	17
MSC D14	*RPL37A*	*IGFBP2*	2	2
MSC D14	*RP3-508I15.19*	*GTPBP1*	22	22
MSC D14	*KCNK6*	*CATSPERG*	19	19
MSC D14	*KDELR1*	*GRIN2D*	19	19
MSC D14	*SLC29A1*	*HSP90AB1*	6	6
MSC D14	*CD81*	*TSSC4*	11	11
MSC D14	*UBE2J2*	*FAM132A*	1	1
MSC D14	*PABPC1P3*	*SNX31*	X	8
MSC D14	*PTGR1*	*BBS5*	9	2
MSC D14	*FZD4*	*RP11-736K20.5*	11	11
MSC D14	*UBE2J2*	*FAM132A*	1	1
MSC D22	*AVIL*	*MARS*	12	12
MSC D22	*SMAD2*	*AC004066.1*	18	4
MSC D22	*PAX3*	*FOXO1*	2	13
MSC D26	*EDF1*	*PHPT1*	9	9
MSC D26	*7SK.206*	*STX3*	11	11
MSC D26	*RP11-316I3.1*	*RP11-316I3.2*	1	1
MSC D26	*FOXC2*	*FOXL1*	16	16
MSC D26	*RP11-458D21.1*	*DDAH1*	1	1
MSC D26	*KDELR1*	*GRIN2D*	19	19
MSC D26	*STEAP2*	*C7orf63*	7	7
MSC D26	*SMG5*	*PAQR6*	1	1
MSC D26	*7SK.206*	*STX3*	11	11
MSC D26	*RP11-312O7.2*	*SRGAP2*	1	1
MSC D26	*7SK.206*	*STX3*	11	11
MSC D26	*RP11-92A5.2*	*NPY2R*	4	4
MSC D26	*RP5-1182A14.1*	*DDAH1*	1	1
MSC D26	*MT-ND6*	*MT-ND4*	MT	MT

NOTE: Three fusions detected at two time points are highlighted. Multiple entries with same parental genes are due to various forms of the fusions.

Published OnlineFirst October 2, 2013; DOI: 10.1158/2159-8290.CD-13-0186

Rhabdomyosarcomas are generally considered skeletal muscle tumors, because of their morphologic muscle-like features. However, they can also arise at sites that normally lack skeletal muscle, such as the genitourinary and biliary tract. Despite extensive research, the exact cell of origin is still under debate (20–22). Our data now suggest that the cell of origin for ARMS may be the cells that transiently express *PAX3–FOXO1*. A connection between the production of chimeric *PAX3–FOXO1* RNA during normal development and recombination between the two genes in cancer is more speculative. Nevertheless, such a connection is not unprecedented. At least in some lower organisms, such as various species of ciliates, RNA has been demonstrated to serve as a guide or template for DNA rearrangement (23, 24).

METHODS

Cell Lines and Culture Conditions

Mesenchymal stem cells (MSC-7043L) were obtained from the Tulane University Center for Gene Therapy. Human embryonic stem cell–derived mesenchymal stem cells (hESC-MSC) were obtained from Millipore. These two cells were maintained in MEMα medium with 20% FBS. Adipose stem cells obtained from donors undergoing liposuction performed by Dr. Adam Katz were maintained in DMEM-F12 medium with 10% FBS. The rhabdomyosarcoma cell line RH30 was cultured in RPMI-1640 medium with 10% FBS. It was acquired from Dr. Anindya Dutta's laboratory (University of Virginia). No further authentication was done for the above cell lines. To induce muscle differentiation, cells were plated on 0.5% gelatin-coated plates and fed with Dulbecco's Modified Eagle Medium (DMEM) containing 10% FBS, 0.1 μmol/L dexamethasone and 50 μmol/L hydrocortisone. Half of the medium was replaced every 4 days. Cells were harvested every other day (25).

Clinical Samples

Nine FFPE sections from abortuses were collected. Skeletal muscle tissues were macrodissected, from which RNA was extracted. Fresh-frozen samples of abortuses were collected under approved Institutional Review Board protocol. When identifiable body parts were present, skeletal muscle from limbs was dissected. If not, whole specimens were used. RNA and protein were extracted using mortar–pestle grinding in the presence of liquid N_2.

NanoString nCounter

The NanoString nCounter system is a fluorescence-based platform to detect individual mRNA molecules without reverse transcription and PCR amplification (10, 26). In this system, each capture probe and reporter probe together query a contiguous region of approximately 100 bp and will hybridize to the target mRNA. RNA was extracted using TRIzol and further purified with the RNeasy Kit (Qiagen). RNA lysates were hybridized to the probe set, incubated overnight at 65°C, washed, eluted according to the nCounter Prep Station manual, and counted by the nCounter Digital Analyzer. The raw data were normalized to the nCounter system spike-in positive and negative controls in each sample. The normalized results are further normalized against three reference genes: *ACTB*, *HPRT*, and *RPLP0*.

FISH and Cytogenetic Analysis

Conventional cytogenetic analysis was performed using standard procedures as follows: cultures were initiated on 22-mm glass coverslips and incubated at 37°C in media consisting of MEM supplemented with FBS, penicillin/streptomycin, and L-glutamine. The cultures were examined daily and harvested as soon as adequate metaphase cells were present. The harvesting consisted of treatment with a 0.4% KCl hypotonic solution followed by fixation with 3:1 methanol:acetic acid. The coverslips for the conventional analysis were treated with 0.01% trypsin followed by Giemsa staining. Cells were examined using an Olympus bright field microscope. For both bone marrow and adipose-derived adult stem cells, 7 cells were analyzed and an additional 13 cells were scored for a total of 20 cells. Coverslips for FISH, harvested in the identical manner as described, were hybridized using standard procedures with the LSI FOXO1 (FOXO1, 13q14) break-apart probe set (Abbott). This probe set consists of a centromere-proximal green segment of 720 kb and a distal red segment of 650 kb. The normal, undisrupted signal is seen as a yellow signal or overlapping red and green signals. Disruptions of the region result in separate red and green signals. A total of 200 interphase nuclei were scored for disruption of the probe set for each cell line. A total of 100 nuclei were scored in a negative control and 50 in a positive control. For frozen sections of fetal muscle samples, at least 1,500 cells were scored on each slide.

Fusion RNA Detection

RNA-seq was performed by Axeq. Briefly, the mRNA in total RNA was converted into a library of template molecules suitable for subsequent cluster generation using the reagents provided in the Illumina TruSeq RNA Sample Preparation Kit. Paired-end sequencing was then conducted using Hiseq 2000 (Illumina). The 101-bp RNA-seq data were then analyzed as described previously (27). For the detection of fusion genes, we used defuse as described before (15). The circular image results of alignments were presented using Circos (28).

Disclosure of Potential Conflicts of Interest

No potential conflicts of interest were disclosed.

Authors' Contributions

Conception and design: H. Yuan, J. Sklar, H. Li
Development of methodology: H. Yuan, F. Qin, M. Movassagh, H. Li
Acquisition of data (provided animals, acquired and managed patients, provided facilities, etc.): H. Yuan, H. Park, H. Li
Analysis and interpretation of data (e.g., statistical analysis, biostatistics, computational analysis): H. Yuan, F. Qin, M. Movassagh, H. Park, W. Golden, Z. Xie, P. Zhang, H. Li
Writing, review, and/or revision of the manuscript: H. Yuan, F. Qin, M. Movassagh, J. Sklar, H. Li
Administrative, technical, or material support (i.e., reporting or organizing data, constructing databases): H. Yuan, W. Golden, Z. Xie, P. Zhang, H. Li
Study supervision: H. Yuan, H. Li

Acknowledgments

The authors thank Dr. Adam Katz for kindly providing the adipose-derived stem cells, Drs. Carola Ponzetto and Riccardo Taulli for providing the pBABE–PAX3–FOXO1 construct, and Dr. Liang Cao for providing the PFM2 antibody. The authors also thank Elizabeth Harker and Brian Reon for their technical support and the University of Virginia Biorepository & Tissue Research Facility for acquiring abortus samples.

Grant Support

H. Li was supported by a Stand up to Cancer Innovation Research Grant, a Program of the Entertainment Industry Foundation (SU2C-AACR-IRG0409); and a V Foundation Scholarship.

Received April 24, 2013; revised September 23, 2013; accepted September 26, 2013; published OnlineFirst October 2, 2013.

Published OnlineFirst October 2, 2013; DOI: 10.1158/2159-8290.CD-13-0186

REFERENCES

1. Rowley JD. The role of chromosome translocations in leukemogenesis. Semin Hematol 1999;36:59–72.
2. Heim S, Mitelman F. Molecular screening for new fusion genes in cancer. Nat Genet 2008;40:685–6.
3. Li H, Wang J, Mor G, Sklar J. A neoplastic gene fusion mimics trans-splicing of RNAs in normal human cells. Science 2008;321:1357–61.
4. Velusamy T, Palanisamy N, Kalyana-Sundaram S, Sahasrabuddhe AA, Maher CA, Robinson DR, et al. Recurrent reciprocal RNA chimera involving YPEL5 and PPP1CB in chronic lymphocytic leukemia. Proc Natl Acad Sci U S A 2013;110:3035–40.
5. Zhang Y, Gong M, Yuan H, Park HG, Frierson HF, Li H. Chimeric transcript generated by cis-splicing of adjacent genes regulates prostate cancer cell proliferation. Cancer Discov 2012;2:598–607.
6. Barr FG, Galili N, Holick J, Biegel JA, Rovera G, Emanuel BS. Rearrangement of the PAX3 paired box gene in the paediatric solid tumour alveolar rhabdomyosarcoma. Nat Genet 1993;3:113–7.
7. Galili N, Davis RJ, Fredericks WJ, Mukhopadhyay S, Rauscher FJ III, Emanuel BS, et al. Fusion of a fork head domain gene to PAX3 in the solid tumour alveolar rhabdomyosarcoma. Nat Genet 1993;5:230–5.
8. Rodriguez-Perales S, Martinez-Ramirez A, de Andres SA, Valle L, Urioste M, Benitez J, et al. Molecular cytogenetic characterization of rhabdomyosarcoma cell lines. Cancer Genet Cytogenet 2004;148:35–43.
9. Cao L, Yu Y, Bilke S, Walker RL, Mayeenuddin LH, Azorsa DO, et al. Genome-wide identification of PAX3-FKHR binding sites in rhabdomyosarcoma reveals candidate target genes important for development and cancer. Cancer Res 2010;70:6497–508.
10. Geiss GK, Bumgarner RE, Birditt B, Dahl T, Dowidar N, Dunaway DL, et al. Direct multiplexed measurement of gene expression with color-coded probe pairs. Nat Biotechnol 2008;26:317–25.
11. Kikuchi K, Tsuchiya K, Otabe O, Gotoh T, Tamura S, Katsumi Y, et al. Effects of PAX3-FKHR on malignant phenotypes in alveolar rhabdomyosarcoma. Biochem Biophys Res Commun 2008;365:568–74.
12. Fredericks WJ, Galili N, Mukhopadhyay S, Rovera G, Bennicelli J, Barr FG, et al. The PAX3-FKHR fusion protein created by the t(2;13) translocation in alveolar rhabdomyosarcomas is a more potent transcriptional activator than PAX3. Mol Cell Biol 1995;15:1522–35.
13. Graf Finckenstein F, Shahbazian V, Davicioni E, Ren YX, Anderson MJ. PAX-FKHR function as pangenes by simultaneously inducing and inhibiting myogenesis. Oncogene 2008;27:2004–14.
14. Khan J, Bittner ML, Saal LH, Teichmann U, Azorsa DO, Gooden GC, et al. cDNA microarrays detect activation of a myogenic transcription program by the PAX3-FKHR fusion oncogene. Proc Natl Acad Sci U S A 1999;96:13264–9.
15. McPherson A, Hormozdiari F, Zayed A, Giuliany R, Ha G, Sun MG, et al. deFuse: an algorithm for gene fusion discovery in tumor RNA-Seq data. PLoS Comput Biol 2011;7:e1001138.
16. Dinger ME, Amaral PP, Mercer TR, Mattick JS. Pervasive transcription of the eukaryotic genome: functional indices and conceptual implications. Brief Funct Genomic Proteomic 2009;8:407–23.
17. Gingeras TR. Implications of chimaeric non-co-linear transcripts. Nature 2009;461:206–11.
18. Downing JR, Khandekar A, Shurtleff SA, Head DR, Parham DM, Webber BL, et al. Multiplex RT-PCR assay for the differential diagnosis of alveolar rhabdomyosarcoma and Ewing's sarcoma. Am J Pathol 1995;146:626–34.
19. Sorensen PH, Lynch JC, Qualman SJ, Tirabosco R, Lim JF, Maurer HM, et al. PAX3-FKHR and PAX7-FKHR gene fusions are prognostic indicators in alveolar rhabdomyosarcoma: a report from the children's oncology group. J Clin Oncol 2002;20:2672–9.
20. Charytonowicz E, Cordon-Cardo C, Matushansky I, Ziman M. Alveolar rhabdomyosarcoma: is the cell of origin a mesenchymal stem cell? Cancer Lett 2009;279:126–36.
21. Keller C, Hansen MS, Coffin CM, Capecchi MR. Pax3:Fkhr interferes with embryonic Pax3 and Pax7 function: implications for alveolar rhabdomyosarcoma cell of origin. Genes Dev 2004;18:2608–13.
22. Hettmer S, Wagers AJ. Muscling in: uncovering the origins of rhabdomyosarcoma. Nat Med 2011;16:171–3.
23. Zaphiropoulos PG. Trans-splicing in higher eukaryotes: implications for cancer development? Front Genet 2011;2:92.
24. Nowacki M, Vijayan V, Zhou Y, Schotanus K, Doak TG, Landweber LF. RNA-mediated epigenetic programming of a genome-rearrangement pathway. Nature 2008;451:153–8.
25. Grigoriadis AE, Heersche JN, Aubin JE. Differentiation of muscle, fat, cartilage, and bone from progenitor cells present in a bone-derived clonal cell population: effect of dexamethasone. J Cell Biol 1988;106:2139–51.
26. Payton JE, Grieselhuber NR, Chang LW, Murakami M, Geiss GK, Link DC, et al. High throughput digital quantification of mRNA abundance in primary human acute myeloid leukemia samples. J Clin Invest 2009;119:1714–26.
27. Ju YS, Kim JI, Kim S, Hong D, Park H, Shin JY, et al. Extensive genomic and transcriptional diversity identified through massively parallel DNA and RNA sequencing of eighteen Korean individuals. Nat Genet 2011;43:745–52.
28. Krzywinski M, Schein J, Birol I, Connors J, Gascoyne R, Horsman D, et al. Circos: an information aesthetic for comparative genomics. Genome Res 2009;19:1639–45.

Published OnlineFirst October 2, 2013; DOI: 10.1158/2159-8290.CD-13-0186

AACR American Association for Cancer Research

CANCER DISCOVERY

A Chimeric RNA Characteristic of Rhabdomyosarcoma in Normal Myogenesis Process

Huiling Yuan, Fujun Qin, Mercedeh Movassagh, et al.

Cancer Discovery 2013;3:1394-1403. Published OnlineFirst October 2, 2013.